Available online at www.sciencedirect.com
ScienceDirect
Trans. Nonferrous Met. Soc. China 33(2023) 507−517
Transactions of Nonferrous Metals Society of China
www.tnmsc.cn

Anomalous eutectic formation in undercooled Ni−P eutectic alloy

Wei LI[1,2,3], Xiu-xun WEI[1,2,3], Jin-fu LI[1,2,3]

1. State Key Laboratory of Metal Matrix Composites, Shanghai Jiao Tong University, Shanghai 200240, China;
2. Shanghai Key Laboratory of Materials Laser Processing and Modification, Shanghai Jiao Tong University, Shanghai 200240, China;
3. School of Materials Science and Engineering, Shanghai Jiao Tong University, Shanghai 200240, China

Received 5 November 2021; accepted 25 March 2022

Abstract: To investigate the relationship between anomalous eutectic and the remelting of primary phase, thin samples of Ni−19.6at.%P eutectic alloy were solidified over a range of undercoolings with temperature recalescence depressed. Fully regular eutectic structures were obtained. The thin samples were then rapidly heated to certain temperatures between the nucleation and eutectic temperatures, resulting in anomalous eutectic structure. It was found that the volume fraction of anomalous eutectic increased with increasing target temperature. α-Ni particulates were in principle randomly oriented while β-Ni_3P phase was well oriented in the anomalous eutectic formed upon heating. Considering that α-Ni is a solid solution while β-Ni_3P is a stoichiometric intermetallic compound, it is unambiguous that anomalous eutectic forms due to remelting of the primary regular eutectic.

Key words: eutectic alloy; undercooling; non-equilibrium solidification; anomalous eutectic; remelting

1 Introduction

Alloy melts solidify at certain undercooling degrees. As the undercooling prior to nucleation increases, a larger driving force for solidification is accumulated. Subsequently, crystals rapidly grow once nuclei form in deeply undercooled melts. Formed far from equilibrium, the solidification structure is considerably different from the conventional one [1−3]. An issue that has been attracting wide attention is the solidification of a eutectic alloy into anomalous eutectic above a critical undercooling [4−9]. Based on the feature that anomalous eutectic is composed of particulates of a eutectic phase dispersing in the other, anomalous eutectic formation was naturally correlated by some researchers with the change in solidification mode. The theories proposed include multiple nucleation of the granular phase ahead of the growing matrix [10,11], decomposition of the primary solid that is highly supersaturated with solute element [4], and decoupled growth of the eutectic phases [5−7,9]. Additionally, GOETZINGER et al [8] thought that the thin lamellar/rod eutectic structure formed in rapid solidification was unstable during the post-recalescence stage due to the large interface energy, and would fragment into the anomalous morphology.

Solidification of undercooled alloy melts proceeds by conducting latent heat of crystallization into the liquid [12−15]. As undercooling increases, the liquid−solid transformation takes place at lower temperature, and the solid is supersaturated with more solute if it is a solid solution [16,17]. On the other hand, the rate of heat dissipation into the environment is far less than the release rate of latent heat of crystallization. Temperature recalescence is thus produced during rapid solidification of highly undercooled alloy melts [18−20]. It is inevitable for

Corresponding author: Jin-fu LI, Tel/Fax: +86-21-54748530, E-mail: jfli@sjtu.edu.cn
DOI: 10.1016/S1003-6326(22)66123-5

part of the primary solid to be remelted in this process. The larger the undercooling is, the more primary solid is remelted [21,22]. In view of this, LI et al [23,24] suggested that remelting plays an important role in anomalous eutectic formation. Such an argument was successively supported by the experimental results of other researchers [7,8,25]. However, it is also argued that anomalous eutectic can be induced by the other reasons, such as the possible kinetic shift in the eutectic point during rapid solidification or the unstable perturbation of interface driven by interfacial energy [26,27]. Thus, the forming mechanism of anomalous eutectic structure in undercooled eutectic alloys is to be resolved.

Ni−19.6at.%P eutectic alloy consists of a solid solution (α-Ni) and a stoichiometric intermetallic compound (Ni_3P) [28−30]. In theory, superheating and remelting can only occur in the solid solution phase. While the stoichiometric intermetallic compound should keep its initial morphology unchanged during this process. Apparently, if the temperature recalescence associated with rapid solidification is fully depressed and the morphology of a primary solid is retained to room temperature, sound evidences for the anomalous eutectic formation can be obtained. In this work, between two fused silica blocks, thin-gauge samples of Ni−19.6at.%P eutectic alloy were solidified at different undercoolings without obvious recalescence, then rapidly heated to higher temperature to simulate the microstructural evolution during the rapid solidification of bulk undercooled alloy. The experimental results clearly indicate that anomalous eutectic forms due to remelting of the primary regular eutectic.

2 Experimental

The Ni−19.6at.%P alloy was produced from 99.999 wt.% electrolytic nickel and 99.9999 wt.% red phosphorus. To reduce the compositional error caused by the volatilization of P during synthesizing the alloy, a Ni−P master alloy with a hypereutectic composition was first prepared. The alloy ingots were gained by further induction melting a mixture of pure Ni and the Ni−P master alloy, covered by a small quantity of B_2O_3 glass flux that had been dehydrated in advance at 1363 K for 2−3 h. Thin-gauge samples for the undercooling experiments were cut from the alloy ingot by wire electrical discharge machining and then ground and polished to ~150 μm in thickness. Figure 1(a) shows a schematic diagram of the experimental apparatus for undercooling the thin-gauge samples. Between two fused silica blocks (the lower one is with a shallow pit), the sample was induction melted in the chamber evacuated to a pressure of 2×10^{-3} Pa and back-filled with ultrapure argon. Then, the sample was cyclically superheated and cooled until a desired undercooling was obtained, during which temperature was also monitored by an infrared pyrometer with an accuracy of 1 K and a response time of 1 ms. The temperature data were recorded in a computer.

To simulate the remelting process of primary solid during temperature recalescence in bulk samples, the thin-gauge samples were heated rapidly at a rate of 300 K/s to different temperatures below the equilibrium eutectic temperature (1163 K) in a Gleeble3500 thermal simulator. Part of the phase diagram of Ni−P binary alloys is shown in Fig. 1(b). Temperature was measured and controlled through a K-type thermocouple welded to the sample. The power supply of the thermal simulator was turned off once the defined temperature was reached and the sample was quickly cooled to room temperature. The samples were polished and etched with a mixture of nitric acid and water. Their microstructures were observed using an optical microscope (OM) equipped with image analysis software and a JSM7800F field emission gun scanning electron microscope (SEM). The orientation distribution of a given phase was investigated by electron-backscattered diffraction (EBSD) in the SEM using HKL EBSD system and CHANNEL 5 software.

3 Results

In the absence of a molten glass flux during melting and solidification, the undercooling achievable in the thin-gauge samples was not more than 65 K. As shown in Figs. 2(a) and (b), the microstructure of the thin-gauge sample is fully composed of rod eutectic, indicating that regular eutectic growth occurred throughout the entire solidification. As expected, the microstructure of regular eutectic formed at 65 K undercooling is

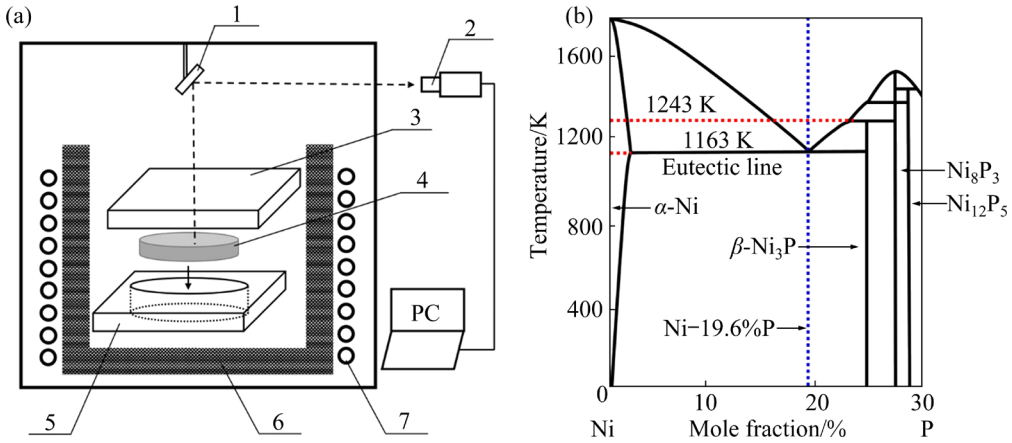

Fig. 1 Schematic diagram of experimental apparatus for undercooling thin-gauge samples (a), and partial phase diagram of Ni−P binary alloys (b) (1−Glass mirror; 2−Infrared pyrometer; 3−Quartz plate; 4−Alloy sample; 5−Quartz crucible; 6−Graphite sleeve; 7−Induction coil)

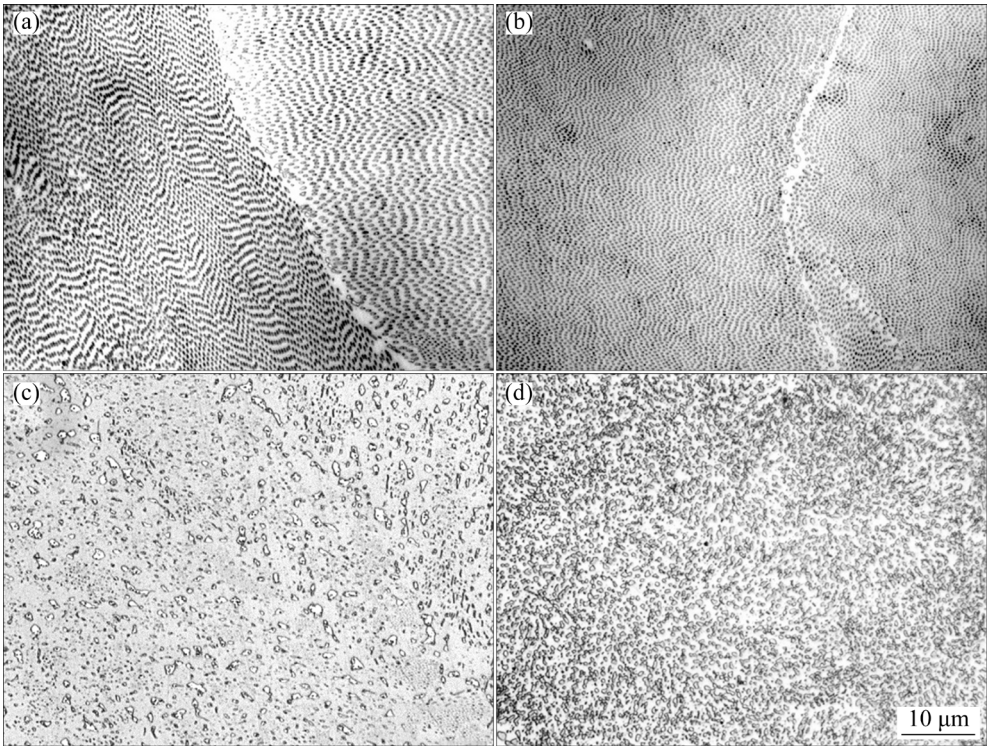

Fig. 2 OM images of microstructures of thin-gauge (a, b) and bulk Ni−P eutectic alloy (c, d) samples solidified at 40 K (a, c) and 65 K (b, d) undercooling

finer than that at 40 K undercooling. Figures 2(c) and (d) show the microstructure of bulk Ni−19.6at.%P eutectic alloy solidified at 40 and 65 K undercooling respectively. Evidently, anomalous eutectic formed in the bulk samples. The microstructure is composed of uniform anomalous eutectic at 65 K undercooling while some regular eutectic is still present at 40 K, indicating that a larger undercooling is advantageous to the anomalous eutectic formation. Noting that the main difference between the bulk and corresponding thin samples with the same undercooling is that the former solidified with temperature recalescence while the latter did not, thus anomalous eutectic formation is closely related with the temperature recalescence.

On rapid heating of the solidified thin-gauge samples, two arrests were observed on the heating curve. Figure 3 shows the heating curve of the sample undercooled by 65 K. The first arrest occurs

at ~1101 K. The second arrest is ~1166 K and slightly higher than the eutectic temperature (1163 K [29]).

If the rapid heating was terminated below the first arrest temperature, there was no noticeable change in the microstructure to be observed. However, the microstructure degenerated when the sample was heated to a temperature between the two arrests. In this case the microstructure was composed of rod eutectic and anomalous eutectic. Figures 4 and 5 show the microstructures of the samples that solidified at undercooling of 40 and 64 K, respectively, and then heated to different temperatures. One can see that the volume fraction of anomalous eutectic increases with increasing target temperature of heating. Further, increasing the initial undercooling results in more anomalous eutectic for a sample heated to a given temperature (Figs. 4(a) and Fig. 5(c)).

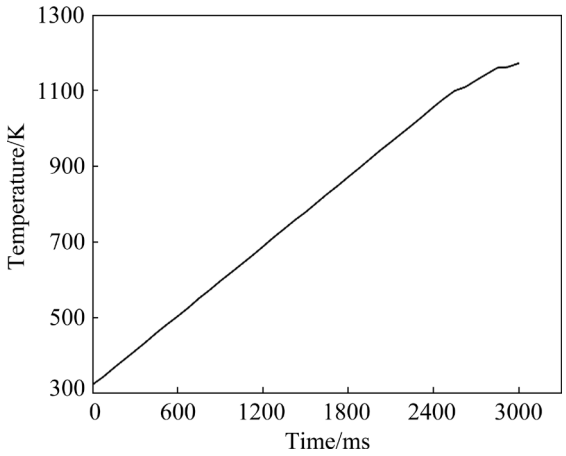

Fig. 3 Rapid heating curve of thin-gauge sample solidified at 65 K undercooling

The heating-induced anomalous eutectic was analyzed by EBSD. The orientation distribution of the phases after heating becomes worse with increasing target temperature. Figure 6 shows EBSD data of the thin samples solidified at 40 K undercooling and heated to 1143 K. Figure 6(a) shows the EBSD pattern when α-Ni and Ni_3P phases are indexed simultaneously. Figures 6(b) and (c) show the patterns when α-Ni and Ni_3P are indexed separately. In the EBSD map of α-Ni, the grains have different colors. In the corresponding partial inverse pole figure (IPF), however, the diffraction direction is mainly localized in a small region (Fig. 6(d)). At the same time, the Ni_3P phase only exhibits a blue color in the EBSD pattern, and its diffraction direction is localized at a point in the partial IPF (Fig. 6(e)). Figures 6(f) and (g) display the distributions of misorientation angle among the α-Ni grains and the Ni_3P matrix in the selected area, respectively, where the theoretical random

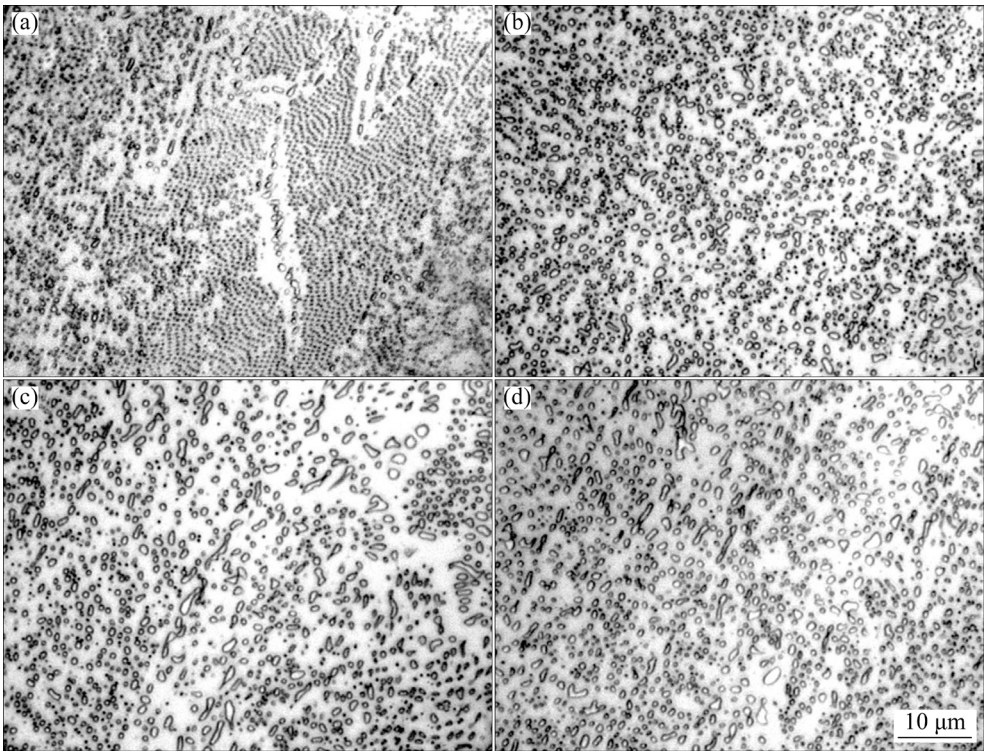

Fig. 4 OM images of thin-gauge sample solidified at 40 K undercooling and rapidly heated to 1133 K (a), 1143 K (b), 1153 K (c) and 1158 K (d)

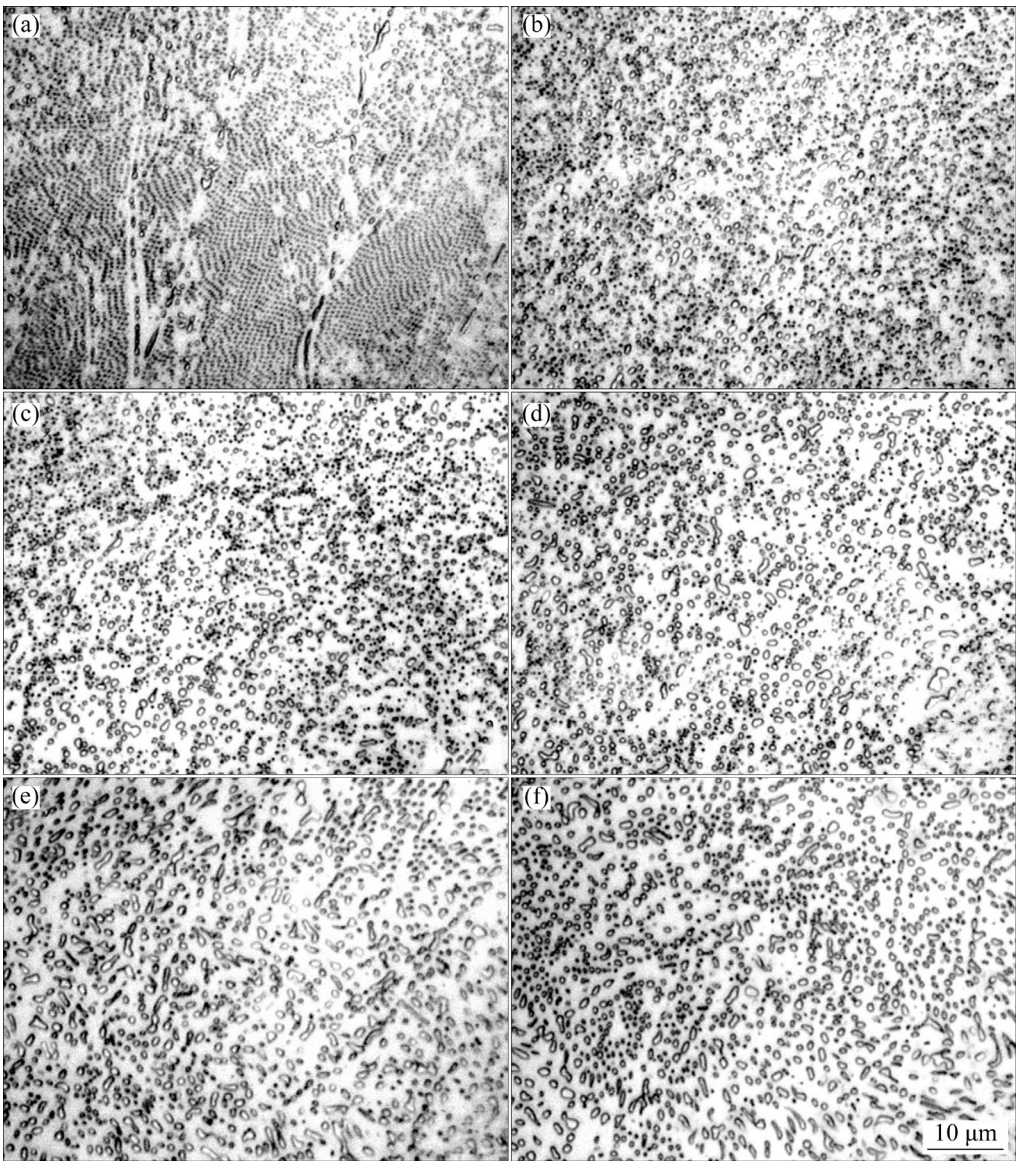

Fig. 5 OM images of thin-gauge sample solidified at 65 K undercooling and rapidly heated to 1113 K (a), 1123 K (b), 1133 K (c), 1143 K (d), 1153 K (e) and 1158 K (f)

distribution curve is also presented. Most of the misorientation angles of the α-Ni grains are below 20°. For the Ni_3P phase, the misorientation angle is near to zero. These results indicate that α-Ni is slightly disorientated, while Ni_3P is completely orientated in the anomalous eutectic.

Figure 7 shows EBSD data of the thin samples after solidification at 40 K undercooling but heated to 1158 K. Compared with the sample heated to 1143 K, the diffraction directions of α-Ni grains are scattered in a larger area in the IPF, while the β-Ni_3P matrix is still oriented to a single direction. The diagram of misorientation angle distribution of α-Ni grains shows a broad peak between 0° and 50°. In contrast, the misorientation angle of the β-Ni_3P matrix is near to zero. Comparing the IPFs and the misorientation angle distributions heated to different temperatures, it is known that the orientation of α-Ni in the eutectic becomes more randomly distributed with increasing heating temperature.

Figures 8 and 9 show the EBSD data of the sample solidified at 65 K undercooling but also heated to 1143 and 1158 K, respectively. Elevating the heating temperature also results in more random distribution of α-Ni grains. Comparing Figs. 6 and 8, and Figs. 7 and 9, it is evident that the orientation of α-Ni phase becomes more random after the undercooling is increased from 40 to 65 K. The misorientation angle of α-Ni phase is very close

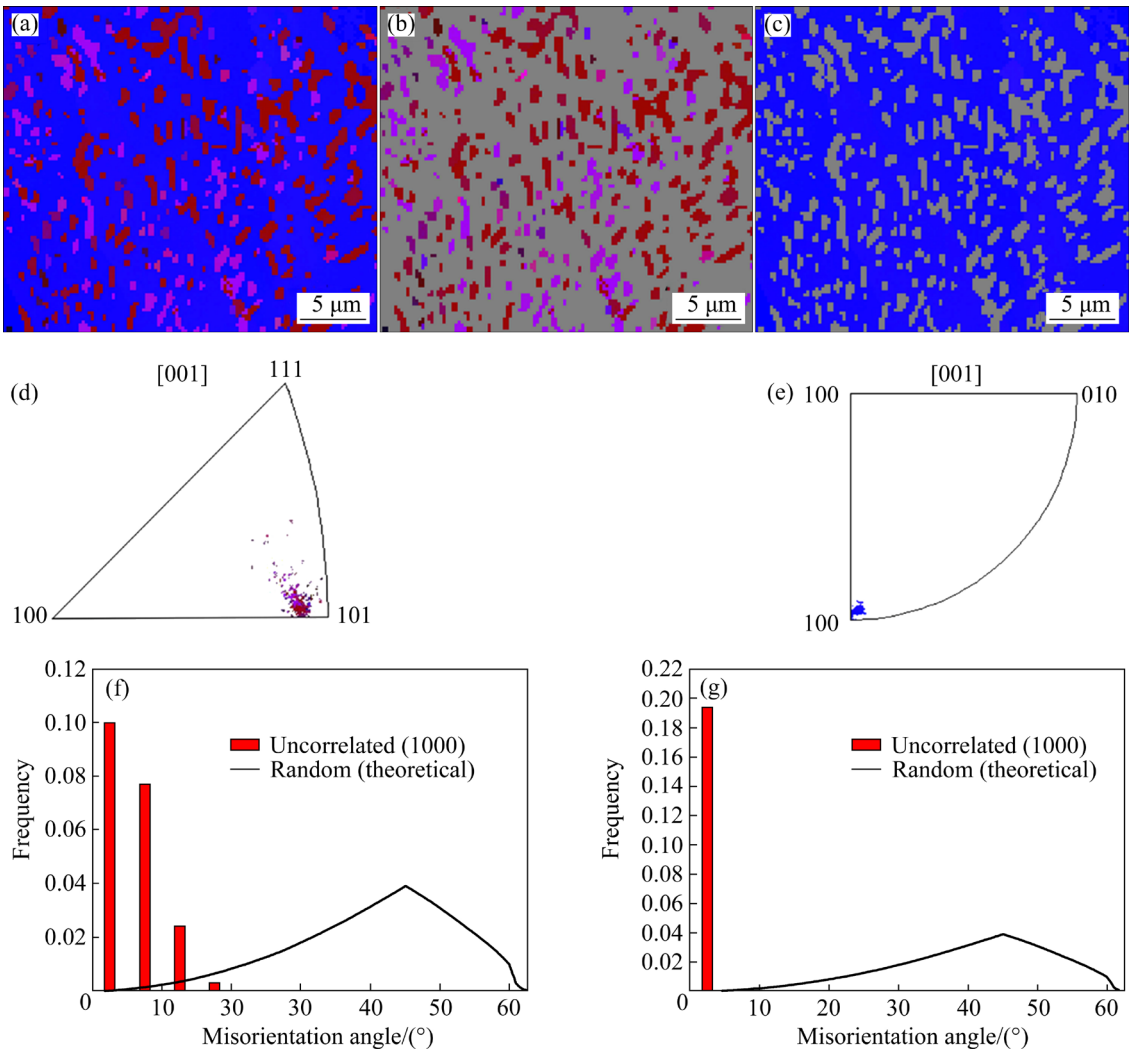

Fig. 6 EBSD measurement of thin-gauge sample solidified at 40 K undercooling and rapidly heated to 1143 K: IPF maps of α-Ni + Ni_3P (a), α-Ni (b) and Ni_3P (c); IPFs of α-Ni (d) and Ni_3P (e); misorientation angle distributions of α-Ni (f) and Ni_3P (g)

to the theoretical random distribution in the sample solidified at 65 K and heated to 1158 K (Fig. 9(f)). Invariably, the β-Ni_3P matrix is completely oriented.

4 Discussion

4.1 Solidification mode

Below the equilibrium eutectic temperature, it is thermodynamically permitted for two eutectic phases to grow cooperatively or separately. Which kind of growth will first occur, according to the current points of view, depends on their relative growth velocities [31,32]. If the coupled growth velocity is higher than that for either of the phases to grow in a decoupled mode, coupled eutectic growth occurs. Otherwise, decoupled growth happens.

Among the eutectic phases of Ni−19.6at.%P alloy, α-Ni has a rapid growth kinetics, while β-Ni_3P, as an intermetallic compound, has a sluggish kinetics especially considering that it has a stoichiometric composition [29,30]. So, α-Ni rather than β-Ni_3P should grow as the primary phase once decoupled growth occurs. The experiment on bulk Ni−19.6at.%P alloy indicated that there was only one recalescence event to take place below a critical undercooling of 117 K but two recalescence events at larger undercoolings [33]. In combination with the microstructural analysis, it has been inferred that coupled eutectic growth of α-Ni and β-Ni_3P occurs throughout the solidification of bulk

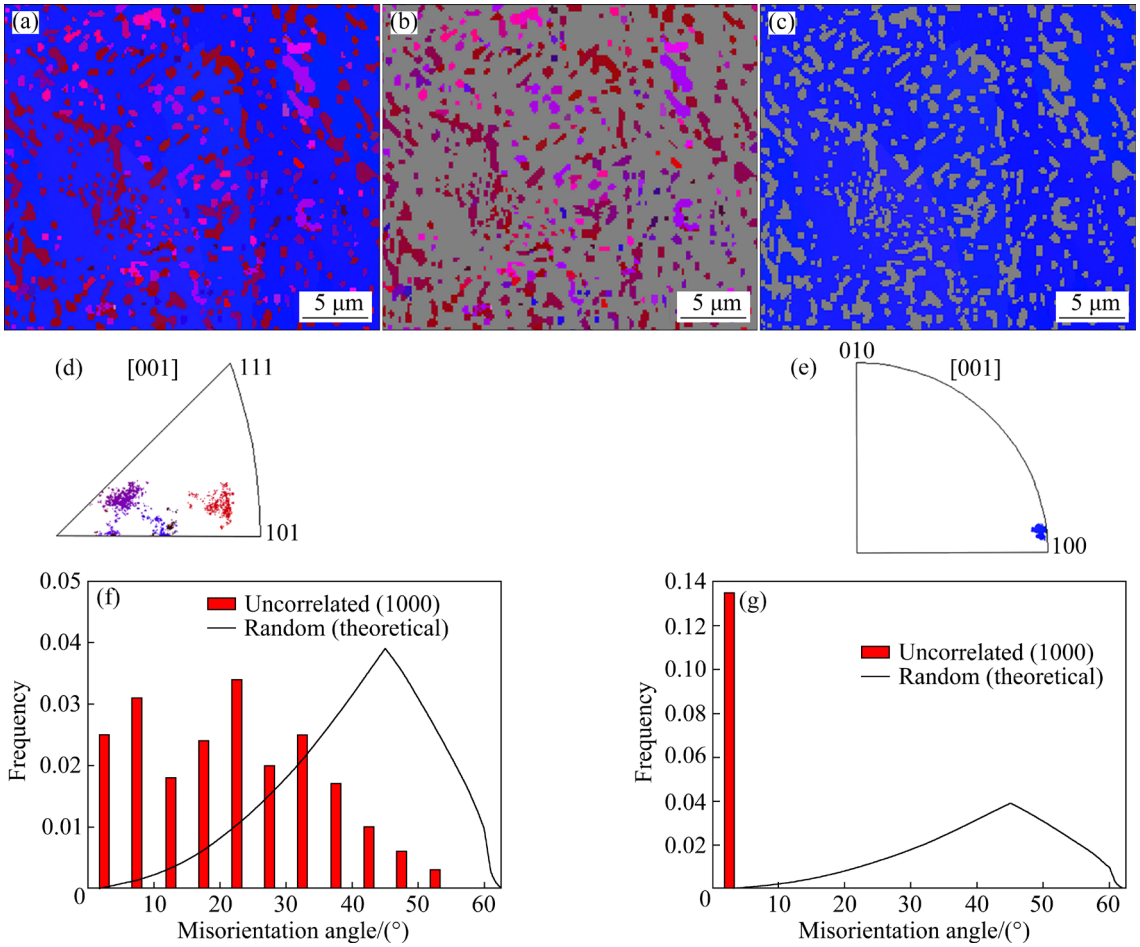

Fig. 7 EBSD measurement of thin-gauge sample solidified at 40 K undercooling and rapidly heated to 1158 K: IPF maps of α-Ni+Ni_3P (a), α-Ni (b) and Ni_3P (c); IPFs of α-Ni (d) and Ni_3P (e); misorientation angle distributions of α-Ni (f) and Ni_3P (g)

Ni−19.6at.%P eutectic melt below 117 K undercooling, while α-Ni solidifies as primary phase at larger undercooling [33]. The present experiment on thin-gauge Ni−19.6at.%P samples irrefutably supported the argument that Ni−19.6at.%P eutectic melt solidified through coupled eutectic growth when undercooling was less than the critical value.

4.2 Mechanism of formation of anomalous eutectic

The driving force for nucleation increases with increasing undercooling. However, it has been turned out that the rise of crystal growth velocity at larger undercooling is more pronounced. The point of view that multiple nucleation of eutectic phases should be responsible for anomalous eutectic formation can be excluded from consideration. This argument is in agreement with the observation that only rod eutectic exists in the thin-gauge samples of Ni−19.6at.%P eutectic alloy. The theory that decoupled growth of eutectic phases results in anomalous eutectic formation can be denied as well.

The prerequisite for a primary solid to be remelted during temperature recalescence is that the primary solid is supersaturated with solute [28]. For the eutectic alloys consisting of two solid solutions, such as Ag−39.9at.%Cu, both phases in the primary eutectic are supersaturated with solute, and will be spontaneously remelted. So two phases are in principle randomly oriented in the resultant anomalous eutectic [28]. For the two eutectic phases of Ni−19.6at.%P, β-Ni_3P is a stoichiometric intermetallic compound, meaning that the concentration does not change with undercooling. Therefore, when bulk Ni−19.6at.%P alloy solidifies at undercooling less than 117 K with α-Ni/β-Ni_3P regular eutectic forming as primary solid, α-Ni fibers rather than the β-Ni_3P matrix break during

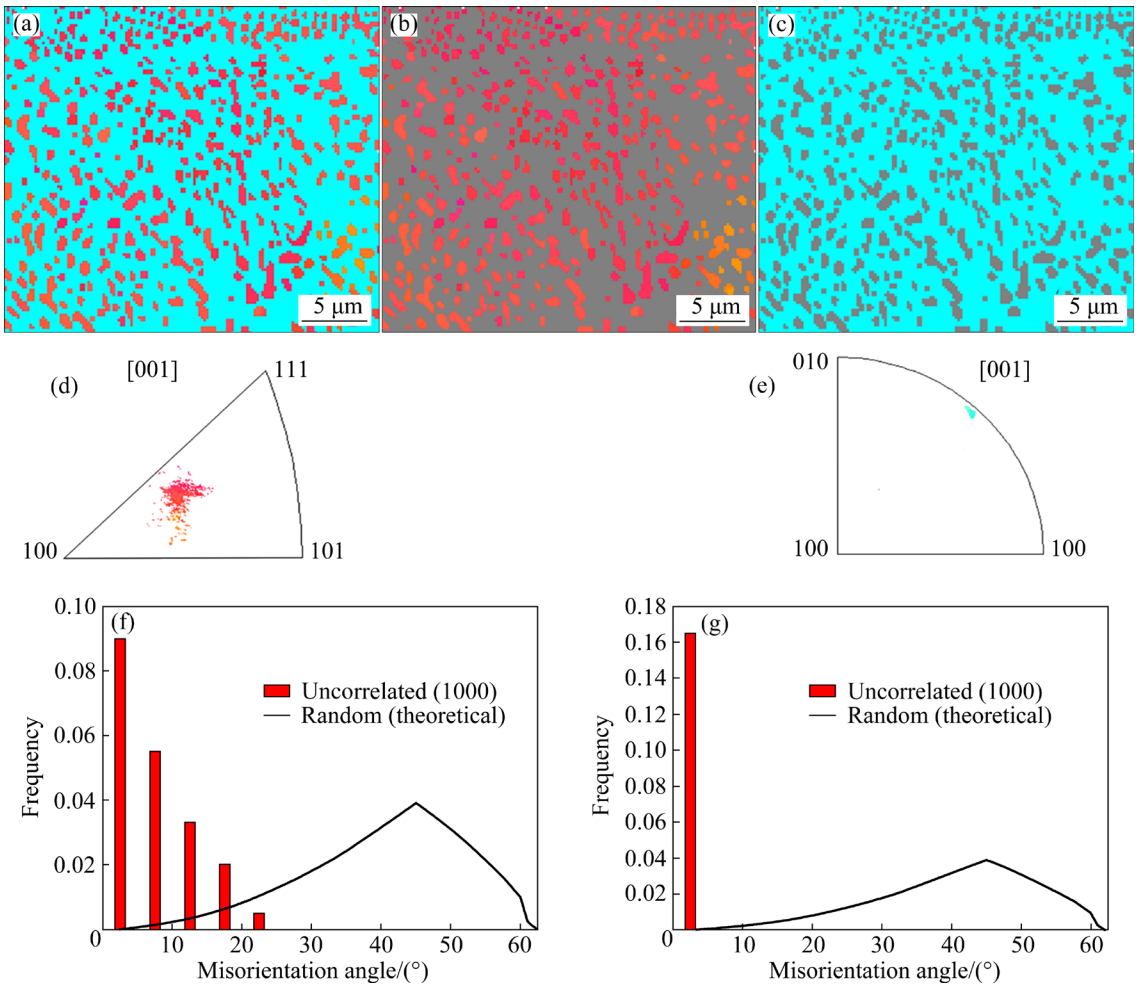

Fig. 8 EBSD measurement of thin-gauge sample solidified at 65 K undercooling and rapidly heated to 1143 K: IPF maps of α-Ni+Ni_3P (a), α-Ni (b) and Ni_3P (c); IPFs of α-Ni (d) and Ni_3P (e); misorientation angle distributions of α-Ni (f) and Ni_3P (g)

temperature recalescence due to superheating and remelting. Consequently, α-Ni particulates are unconnected but the β-Ni_3P matrix is continuous in the anomalous eutectic. The broken α-Ni crystals can rotate by an angle during solidification, making the misorientation angles among them enlarge. While the β-Ni_3P phase is always well oriented in the microstructure even if the sample has undergone a complicated thermal history. The larger the undercooling prior to nucleation is or the higher temperature the sample is reheated to, the more solid is remelted during heating. So more anomalous eutectic forms and α-Ni particulates are more randomly distributed in the anomalous eutectic, as shown in Figs. 6−9. This is also why the sample solidified at 65 K undercooling has shown anomalous eutectic structure when it is heated to such low temperatures as 1113 and 1123 K. In addition, if the theory that anomalous eutectic formation is driven by the solid-solid interface energy was correct, both α-Ni and β-Ni_3P phases should be well oriented in the anomalous eutectic. But the fact is not so. All the experimental results of the thin-gauge Ni−19.6at.%P samples confirm that the anomalous eutectic results from the partial remelting of the primary α-Ni/β-Ni_3P rod eutectic when the alloy solidifies at undercooling below 117 K.

Different from bulk samples in which rapid solidification and resultant solute supersaturation only occur in part of the solid (the primary solid, for example, the branching stems in the case of dendritic growth) while the other part solidifies under a near-equilibrium condition, the thin-gauge samples placed between two fused silica blocks solidifies without temperature recalescence. Namely,

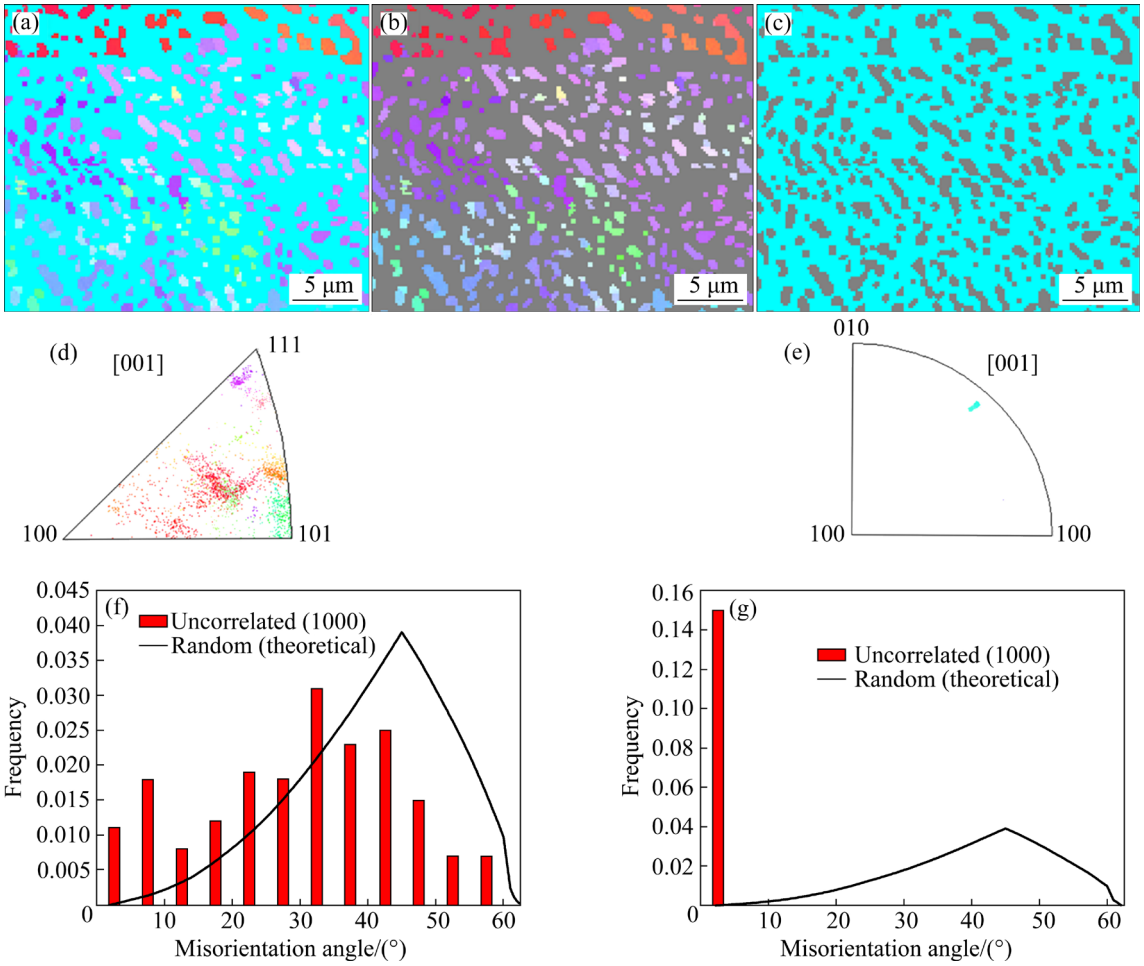

Fig. 9 EBSD measurement of thin-gauge sample solidified at 65 K undercooling and rapidly heated to 1158 K: IPF maps of α-Ni+Ni_3P (a), α-Ni (b) and Ni_3P (c); IPFs of α-Ni (d) and Ni_3P (e); misorientation angle distributions of α-Ni (f) and Ni_3P (g)

all the solid forms at nearly the same undercooling (temperature) and has the same supersaturation of solute everywhere. When such samples are subjected to heating, remelting should take place in the whole sample, and anomalous eutectic formation is not confined to special areas, as shown in Figs. 4 and 5.

A transition from coupled to decoupled growth of eutectic phases at large undercooling widely occurs in eutectic alloys [7,24,34,35]. The anomalous eutectic formation at large undercooling is also related with the remelting of the primary phase [23]. But limited by the undercooling achieved in the thin sample, it is infeasible to verify the related mechanism using the present method.

5 Conclusions

(1) The temperature recalescence during solidification of undercooled alloy melts can be effectively depressed by using ~150 μm-thick samples sandwiched between fused silica blocks. This casting method generates a fully rod eutectic regardless of the degree of undercooling up to 65 K. Rapidly heating the sample at 300 K/s to a target temperature in the vicinity of the eutectic temperature results in formation of anomalous eutectic in the re-cooled microstructure, whereby its fraction increases with increasing heating temperature.

(2) α-Ni particulates are in principle randomly oriented while β-Ni_3P phase is well oriented in the anomalous eutectic in the reheated thin-gauge samples.

(3) It is verified that partial remelting of primary regular eutectic can result in anomalous eutectic formation even though the primary eutectic only includes one solid solution phase.

Acknowledgments

This work was supported by the National Natural Science Foundation of China (Nos. 51771116, 51620105012, 51821001).

References

[1] YANG Chang-lin, YANG Gen-cang, LU, Yi-ping, CHEN Yu-zeng, ZHOU Yao-he. Phase selection in highly undercooled Fe−B eutectic alloy melts [J]. Transactions of Nonferrous Metals Society of China, 2006, 16(1): 39−43.

[2] LIU Li, MA Xiao-li, HUANG Qi-sen, LI Jin-fu, CHENG Xian-hua, ZHOU Yao-he. Solidification process and microstructure evolution of bulk undercooled Co−Sn alloys [J]. Transactions of Nonferrous Metals Society of China, 2013, 23: 289−293.

[3] ZHAI Wei, CHANG Jian, GENG De-lu, WEI Bing-bo. Progress and prospect of solidification research for metallic materials [J]. The Chinese Journal of Nonferrous Metals, 2019, 29(9): 1953−2008. (in Chinese)

[4] KATTAMIS T Z, FLEMINGS M C. Structure of undercooled Ni−Sn eutectic [J]. Metallurgical and Materials Transactions B, 1970, 1: 1449−1451.

[5] JONES B L. Growth mechanisms in undercooled eutectics [J]. Metallurgical Transactions, 1971, 2: 2950−2951.

[6] YAO W J, HAN X J, WEI B. Microstructural evolution during containerless rapid solidification of Ni−Mo eutectic alloys [J]. Journal of Alloys and Compounds, 2003, 348: 88−99.

[7] WEI B, HERLACH D M, FEUERBACHER B, SOMMER F. Dendritic and eutectic solidification of undercooled Co−Sb alloys [J]. Acta Metallurgica et Materialia, 1993, 41: 1801−1809.

[8] GOETZINGER R, BARTH M, HERLACH D M. Mechanism of formation of the anomalous eutectic structure in rapidly solidified Ni−Si, Co−Sb and Ni−Al−Ti alloys [J]. Acta Materialia, 1998, 46:1647−1655.

[9] LI M J, NAGASHIO K, ISHIKAWA T, YODA S, KURIBAYASHI K. Microtexture and macrotexture formation in the containerless solidification of undercooled Ni−18.7at.%Sn eutectic melts [J]. Acta Materialia, 2005, 53: 731−741.

[10] POWELL G L F, HOGAN L M. Undercooling in silver-copper eutectic alloys [J]. Journal of the Institute of Metals, 1965, 93: 505−512.

[11] LI M J, KURIBAYASHI K. Nucleation-controlled microstructures and anomalous eutectic formation in undercooled Co−Sn and Ni−Si eutectic melts [J]. Metallurgical and Materials Transactions A, 2003, 34: 2999−3008.

[12] MULLINS W W, SEKERKA R F. Stability of a planar interface during solidification of a dilute binary alloy [J]. Journal of Applied Physics, 1964, 35: 444−451.

[13] LUDWIG A. Limit of absolute stability for crystal growth into undercooled alloy melts [J]. Acta Metallurgica et Materialia, 1991, 39: 2795−2798.

[14] MULLIS A M, COCHRANE R F. Grain refinement and the stability of dendrites growing into undercooled pure metals and alloys [J]. Journal of Applied Physics, 1997, 82: 3783−3790.

[15] LI J F, YANG G C, ZHOU Y H. Kinetic effect of crystal growth on the absolute stability of a planar interface in undercooled melts [J]. Materials Research Bulletin, 2000, 35: 1775−1783.

[16] MEHRABIAN R, PARRISH P A. Rapid solidification processing: Principles and technologies IV [M]. Baton Rouge, LA: Claitor's Publishing Division, 1988.

[17] LI J F, ZHOU Y H. Eutectic growth in bulk undercooled melts [J]. Acta Materialia, 2005, 53: 2351−2359.

[18] KOSEKI T, FLEMINGS M C. Solidification of undercooled Fe−Cr−Ni alloys: Part I. Thermal behavior [J]. Metallurgical and Materials Transactions A, 1995, 26: 2991−2999.

[19] YANG C L, LIU F, YANG G C, CHEN Y Z, LIU N, ZHOU Y H. Microstructure and phase selection in bulk undercooled Fe−B eutectic alloys [J]. Journal of Alloys and Compounds, 2007, 441: 101−106.

[20] RUAN Y, GU Q Q, LU P, WANG H P, WEI B. Rapid eutectic growth and applied performances of Fe−Al−Nb alloy solidified under electromagnetic levitation condition [J]. Materials and Design, 2016, 112: 239−245.

[21] XU X L, HOU H, ZHAO Y H, LIU F. Nonequilibrium solidification, grain refinements, and recrystallization of deeply undercooled Ni−20at.%Cu alloys: Effects of remelting and stress [J]. Metallurgical and Materials Transactions A, 2017, 48: 4777−4785.

[22] LI J F, ZHOU, Y H. Remelting of primary solid in rapid solidification of deeply undercooled alloy melts [J]. Acta Metallurgica Sinica, 2018, 54: 627−636. (in Chinese)

[23] LI J F, LI X L, LIU L, LU S Y. Mechanism of anomalous eutectic formation in the solidification of undercooled Ni−Sn eutectic alloy [J]. Journal of Materials Research, 2008, 23: 2139−2148.

[24] LI J F, JIE W Q, ZHAO S, ZHOU Y H. Structural evidence for the transition from coupled to decoupled growth in the solidification of undercooled Ni−Sn eutectic melt [J]. Metallurgical and Materials Transactions A, 2007, 38: 1806−1816.

[25] DONG H, CHEN Y Z, WANG K, SHAN G B, ZHANG Z R, ZHANG W X, LIU F. Modeling remelting induced destabilization of lamellar eutectic structure in an undercooled Ni−18.7at.%Sn eutectic alloy [J]. Journal of Alloys and Compounds, 2020, 826: 154018.

[26] MULLIS A M, CLOPET C R. On the origin of anomalous eutectic growth from undercooled melts: Why re-melting is not a plausible explanation [J]. Acta Materialia, 2018, 145: 186−195.

[27] DONG H, CHEN Y Z, ZHANG Z R, SHAN G B, ZHANG W X, LIU F. Mechanisms of eutectic lamellar destabilization upon rapid solidification of an undercooled Ag−39.9at.%Cu eutectic alloy [J]. Journal of Materials Science and Technology, 2020, 59: 173−179.

[28] WEI X X, LIN X, XU W, HUANG Q S, FERRY M, LI J F, ZHOU Y H. Remelting-induced anomalous eutectic formation during solidification of deeply undercooled eutectic alloy melts [J]. Acta Materialia, 2015, 95: 44−56.

[29] HUANG Q S, LIU L, LI J F, LIN F, ZHOU Y H. Redetermination of the eutectic composition of the Ni−P

binary alloy [J]. Journal of Phase Equilibria and Diffusion, 2010, 31: 532−535.
[30] MASSALSKI T B. Binary alloy phase diagrams [M]. 2nd ed. Materials Park, Ohio: ASM International, 1990.
[31] SCHMETTERER C, VIZDAL J, IPSER H. A new investigation of the system Ni−P [J]. Intermetallics, 2009, 17: 826−834.
[32] LI M, NAGASHIO K, KURIBAYASHI K. Reexamination of the solidification behavior of undercooled Ni−Sn eutectic melts [J]. Acta Materialia, 2002, 50: 3241−3252.
[33] HUANG Qi-sen, LIU Li, WEI Xiu-xun, LI Jin-fu. Solidification behaviors of undercooled Ni-P alloys [J]. Acta Physica Sinca, 2012, 61(16): 166401-1−166401-8. (in Chinese)
[34] LUO S B, WANG W L, XIA Z C, WEI B. Theoretical prediction and experimental observation for microstructural evolution of undercooled nickel-titanium eutectic type alloys [J]. Journal of Alloys and Compounds, 2017, 692: 265−273.
[35] LIU F, CHEN Y Z, YANG G C, LU Y P, CHEN Z, ZHOU Y H. Competitions incorporated in rapid solidification of the bulk undercooled eutectic $Ni_{78.6}Si_{21.4}$ alloy [J]. Journal of Materials Research, 2007, 22: 2953−2963.

过冷 Ni−P 共晶合金中反常共晶的形成

李 伟[1,2,3]，韦修勋[1,2,3]，李金富[1,2,3]

1. 上海交通大学 金属基复合材料国家重点实验室，上海 200240；
2. 上海交通大学 上海市材料激光加工与改性重点实验室，上海 200240；
3. 上海交通大学 材料科学与工程学院，上海 200240

摘 要：为研究初生相重熔与反常共晶形成之间的关系，在一定过冷度范围内制备温度再辉被抑制的 Ni−19.6%P (摩尔分数)共晶合金薄片试样，得到完全规则的共晶组织。随后将薄片样品快速加热到介于凝固形核与共晶反应之间的特定温度，观察到反常共晶结构的形成，并且反常共晶组织的体积分数随着加热温度的升高而增大。此外，在快速加热后所获得的反常共晶组织中 α-Ni 的取向随机，而 β-Ni_3P 相则呈现共同的取向。α-Ni 为固溶体，但是 β-Ni_3P 为具有一定化学计量比的金属间化合物，充分说明初生规则共晶的重熔正是反常共晶组织的成因。

关键词：共晶合金；过冷度；非平衡凝固；反常共晶；重熔

(Edited by Xiang-qun LI)